

# Coupled 0D chemical kinetics and 2D fluid dynamics modelling of a plasma jet interacting with water: Reactivity and stability of RONS

A. Bogaerts, P. Heirman and W. Van Boxem

Research group PLASMANT, Department of Chemistry, University of Antwerp, Antwerp, Belgium

**Abstract:** We present a combination of a 0D chemical kinetics model and a 2D fluid dynamics model of the kINPen plasma jet interacting with liquid water, to study the gas and liquid flow behavior, as well as the transport and chemical reactions of reactive oxygen and nitrogen species (RONS) both in gas phase and liquid phase. We calculate (among others) the species concentrations, both during and after plasma treatment, to elucidate the chemical pathways and the lifetime of the various RONS in solution.

**Keywords:** Plasma-liquid interaction, RONS, modelling, chemistry, fluid dynamics

## 1. Introduction

Plasma-treated liquids are gaining increasing interest for cancer treatment and other medical applications [1-3], but their chemistry is not yet fully understood. To get more insight in the reactivity and stability of RONS, both during and after plasma treatment, we have developed a combined 0D chemical kinetics model and axisymmetric 2D fluid dynamics model to describe the interaction of the kINPen plasma jet with liquid water (buffered at pH 7.3, like in PBS), in a well of 2 mL (see Fig. 1).

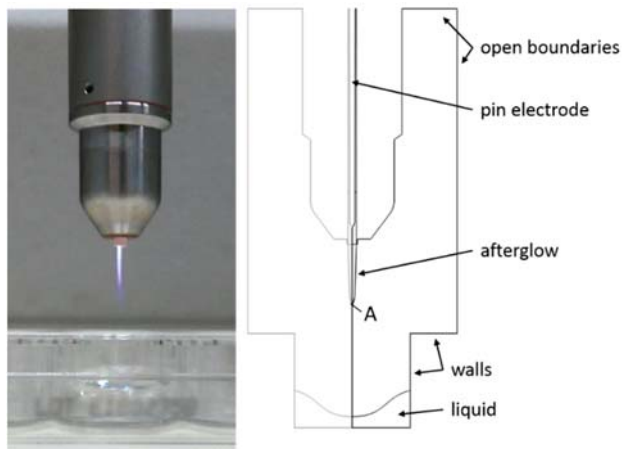


Fig. 1. Photograph of the kINPen treating 2 mL liquid (left) and geometry of the simulated system (right).

## 2. Description of the models

The 0D chemical kinetics model (ZDPlasKin [3]) is based on solving balance equations for the various species, with production and loss terms defined by chemical reactions. The time-dependence of the calculated species densities can be translated into a spatial dependence (i.e., as a function of distance from the pin electrode till the liquid), based on the gas flow velocity. The gas velocity, as well as the gas temperature and the mixing rate of the jet with ambient air, which affects the chemistry, are adopted from our 2D flow simulations. This 0D model provides the detailed chemistry, and is used to define the major species and chemical reactions, to be taken into account in the (much more time-consuming) 2D model. In addition, the plasma species densities at the end of the afterglow are used as input in the 2D model, so that we don't need to

account for electron processes in the latter model, thus reducing its calculation time.

The 2D fluid dynamics model is developed within COMSOL. We calculate the turbulent flow in gas and liquid phase based on the Navier-Stokes equations. Heat transfer is also described, as well as evaporation of water into the gas phase. Transport and chemical reactions of all the species in both gas and liquid phase is calculated by coupled continuity and transport equations. Transport of the species over the gas-liquid interface is determined by Henry's law. The species taken into account in this 2D model are listed in Table 1. These species react with each other, as described by a limited chemistry set of 56 gas phase reactions and 52 liquid phase reactions.

Table 1. Gas and liquid species included in the 2D model.

	Gas phase	Liquid phase
<b>Molecules</b>	O <sub>2</sub> , O <sub>3</sub> , H <sub>2</sub> , HO <sub>2</sub> , H <sub>2</sub> O <sub>2</sub> , H <sub>2</sub> O, N <sub>2</sub> , HNO, HNO <sub>2</sub> , HNO <sub>3</sub> , N <sub>2</sub> O, Ar	O <sub>2</sub> , O <sub>3</sub> , H <sub>2</sub> , HO <sub>2</sub> , H <sub>2</sub> O <sub>2</sub> , N <sub>2</sub> , HNO, HNO <sub>2</sub> , HNO <sub>3</sub> , N <sub>2</sub> O, ONOOH
<b>Radicals</b>	O, H, OH, N, NH, NO, NO <sub>2</sub> , NO <sub>3</sub>	O, H, OH, N, NH, NO, NO <sub>2</sub> , NO <sub>3</sub>
<b>Excited species</b>	O <sub>2</sub> (1D)	
<b>Ions</b>		O <sub>2</sub> <sup>-</sup> , OH <sup>-</sup> , H <sub>3</sub> O <sup>+</sup> , NO <sub>2</sub> <sup>-</sup> , NO <sub>3</sub> <sup>-</sup> , ONOO <sup>-</sup>

## 3. Results and discussion

### 3.1. Gas and liquid flow profiles

Fig. 2 illustrates the calculated steady state flow profile in both gas and liquid phase, for a flow rate of 3 slm argon. This results in a maximum velocity of 57 m/s inside the plasma jet, while the maximum gas velocity outside the plasma jet is 34 m/s. When the gas flow reaches the liquid surface, it flows towards the edge of the well, causing a shear stress on the liquid surface. Upon hitting the edge of the well, the gas flow results in a vortex within the well, so that the gas flows back towards the afterglow. Because of the shear stress on the liquid surface, the upper layer of the liquid starts to move in the same direction as the gas, but with a lower velocity. The maximum velocity in the liquid (2.5 m/s) is reached near the edge of the well. The liquid

movement results in another vortex in the liquid phase (see close-up on Fig. 2).

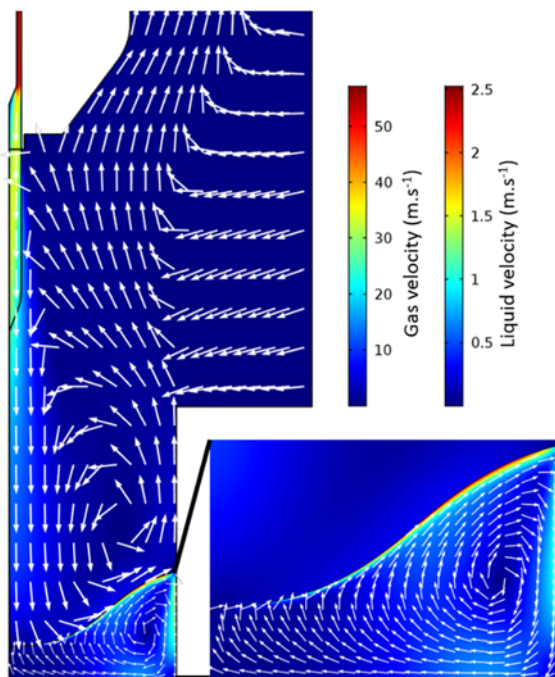


Fig. 2. Steady state gas and liquid flow profiles, for an inlet flow rate of 3 slm argon. The color scale gives the velocity magnitudes, while the arrows show the flow direction.

### 3.2. Gas and liquid phase concentration profiles

In **Fig. 3** we plot the gas phase densities and liquid phase concentrations of the three major RONS, i.e.,  $\text{H}_2\text{O}_2$ ,  $\text{HNO}_2$  and  $\text{HNO}_3$ , after 10 seconds of plasma treatment. The profiles clearly follow the gas and liquid flow profiles. Indeed, convection of species is more important than diffusion. The  $\text{H}_2\text{O}_2$  density is the highest underneath the plasma jet, just above the liquid surface. Its density drops to half its value towards the edge of the well and in the bulk gas.  $\text{HNO}_2$  is only formed to a small extent underneath the plasma jet, just above the liquid surface, but its density is the highest towards the edge of the well. The  $\text{HNO}_3$  density profile does not rise at all underneath the plasma jet. The  $\text{HNO}_2$  and  $\text{HNO}_3$  species accumulate in the vortex in the gas phase.

Transport to the liquid phase is dictated by the Henry's constants, which are above 1 for  $\text{H}_2\text{O}_2$ ,  $\text{HNO}_2$  and  $\text{HNO}_3$ . This means that their equilibrium is towards the liquid phase, as is clear from the difference between gas phase density profile just above the liquid surface, and the liquid phase concentration profile just below the liquid surface (see the close-ups in Fig. 3). The gas phase density of the species is very low just above the liquid surface, because the species are transported towards the liquid, while in the upper layer of the liquid the opposite trend is observed: the liquid concentration is the highest in the first few nm below the liquid surface, because the species enter from the gas phase. The highest concentration of  $\text{H}_2\text{O}_2$  in the liquid is

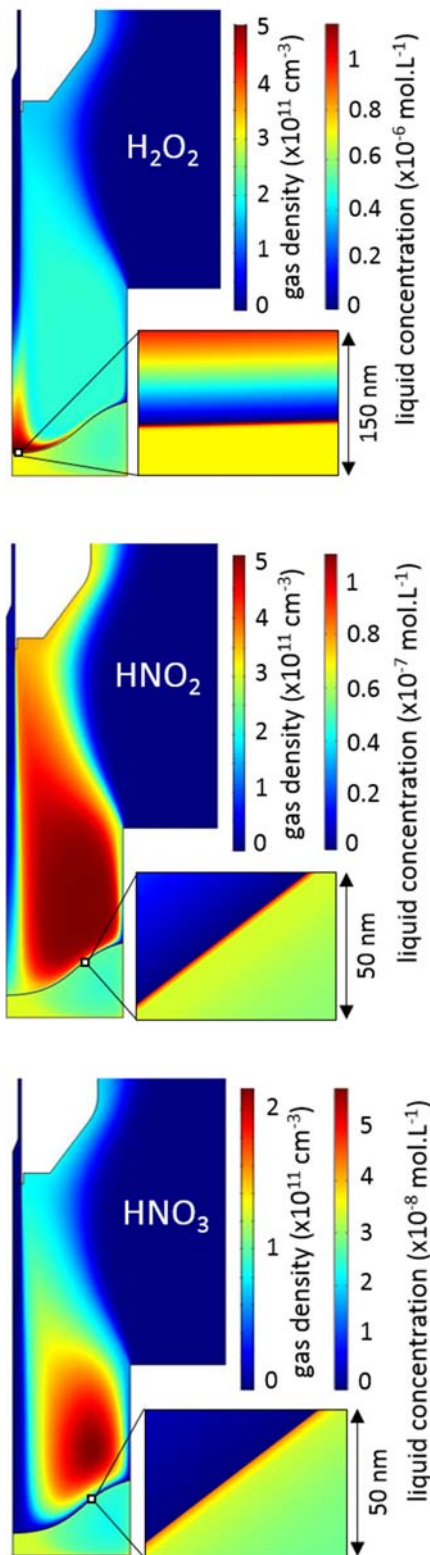
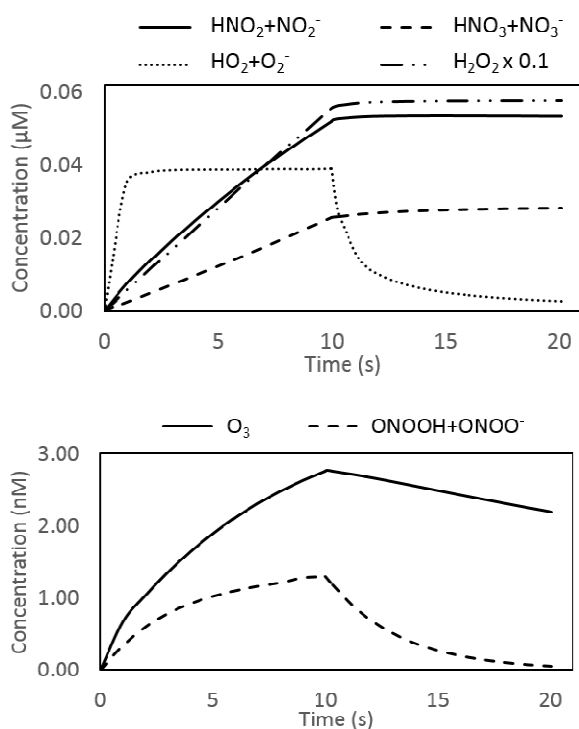


Fig. 3. 2D plots of the gas phase densities and liquid phase concentrations of  $\text{H}_2\text{O}_2$ ,  $\text{HNO}_2$  and  $\text{HNO}_3$ , after 10 seconds of plasma treatment.

calculated to be ten times greater than that of  $\text{HNO}_2$ , which is on its turn ten times greater than that of  $\text{HNO}_3$  (cf. different values in the color scales of Fig. 3).

### 3.3. Stability of the long-lived RONS in the liquid after plasma treatment

**Fig. 4** illustrates the volume-integrated liquid-phase concentrations of the RONS that are able to accumulate in the liquid, so-called long-lived RONS, as a function of time, both during and after plasma treatment, for a plasma treatment time of 10 seconds. During plasma treatment, three different patterns of concentration change with time can be seen. The  $\text{H}_2\text{O}_2$ ,  $\text{HNO}_2$ , and  $\text{HNO}_3$  concentrations increase linearly with time, in agreement with our previous experimental results [4]. The  $\text{HO}_2$  concentration rises very quickly in the first milliseconds, after which it reaches a steady state till the end of the plasma treatment. Finally, the concentrations of  $\text{O}_3$  and  $\text{ONOOH}$  keep on increasing over time, but the rise flattens up as a function of treatment time.



**Fig. 4.** Volume-integrated liquid phase concentrations of the long-lived RONS, as a function of time during and after plasma treatment, for a plasma treatment time of 10 seconds.

After plasma treatment (i.e., after 10 seconds),  $\text{H}_2\text{O}_2$ ,  $\text{HNO}_2$  and  $\text{HNO}_3$  are clearly the only stable species in the liquid. Their concentrations remain constant in the first 10 seconds after plasma treatment, and there is no indication that these concentrations will drop at a later time point. This is also in agreement with our previous experimental data [4], where the  $\text{H}_2\text{O}_2$  and  $\text{HNO}_2$  concentrations did not change in the plasma-treated liquid for up to 2 hours after

plasma treatment ( $\text{HNO}_3$  was not measured). The concentrations of  $\text{HO}_2$ ,  $\text{ONOOH}$ , and  $\text{NO}_2$  drop quickly after plasma treatment, and no significant amount of these species is present after 10 seconds. Finally, the  $\text{O}_3$  concentration decreases linearly after plasma treatment. After 10 seconds, its concentration has dropped to 80% of its value at the end of the plasma treatment. This linear drop can be explained by transport of  $\text{O}_3$  back to the gas phase, because the Henry's constant of  $\text{O}_3$  is lower than 1, which means that its equilibrium is pointed towards the gas phase. According to our simulations, it will take ca. 50 seconds before the  $\text{O}_3$  concentration has dropped to negligible values.

### 3.4. Liquid phase chemistry

All the long-lived RONS presented in Fig. 4, except for  $\text{O}_3$ , have a Henry's constant larger than 1, so they are continuously transported from the gas phase to the liquid phase during plasma treatment. In addition, they also undergo chemical reactions in the liquid, as schematically illustrated in Fig. 5.

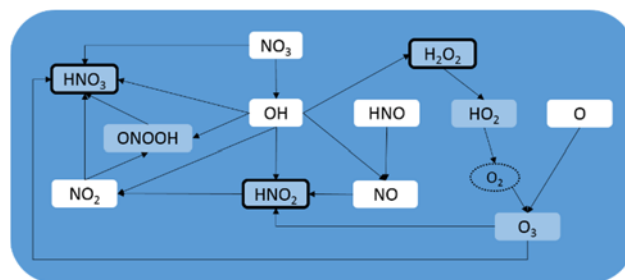


**Fig. 5.** Schematic overview of the most important liquid chemistry. Species in white boxes are short-lived species that completely react away in the first few nm below the liquid surface. Species in blue boxes are able to accumulate in the bulk liquid, but only the species with a black frame are stable in the liquid after plasma treatment.

The liquid chemistry for  $\text{H}_2\text{O}_2$ ,  $\text{HNO}_2$  and  $\text{HNO}_3$  (indicated with black frames in Fig. 5), is mainly driven by reactions of short-lived species, like  $\text{OH}$  and  $\text{NO}_2$ .  $\text{H}_2\text{O}_2$  and  $\text{HNO}_3$  exhibit a net production by chemical reactions, while for  $\text{HNO}_2$  the loss reactions in the liquid are faster than the production reactions. Because the short-lived species are only present in the first few nm below the gas-liquid interface, this is where the only significant changes in liquid concentrations are happening. In addition, because both the production and loss reactions of  $\text{H}_2\text{O}_2$ ,  $\text{HNO}_2$  and  $\text{HNO}_3$  are only based on these very short-lived radicals ( $\text{OH}$ ,  $\text{NO}$ ,  $\text{NO}_2$ ), which will be completely gone immediately after plasma treatment,  $\text{H}_2\text{O}_2$ ,  $\text{HNO}_2$  and  $\text{HNO}_3$  are not being formed or lost anymore in the liquid chemistry (at least not on the short time scales of relevance here). Furthermore, because of their high Henry's constants, they will not (significantly) evaporate into the gas phase. Hence, this explains why their concentrations remain constant after plasma treatment (see Fig. 4).

Although ONOOH, HO<sub>2</sub>, and O<sub>3</sub> are able to accumulate to some extent in the liquid during plasma treatment, their concentrations clearly drop after plasma treatment (see Fig. 4). For ONOOH and HO<sub>2</sub> this is due to more important loss than production reactions in the liquid after treatment, as revealed by our simulations, while O<sub>3</sub> evaporates into the gas phase because of its low Henry's constant

#### 4. Conclusion

The combined 0D chemical kinetics model and 2D fluid dynamics model, which we developed for the kINPen plasma jet interacting with liquid water, gives detailed information on the behavior (i.e., transport and chemical reactions) of RONS, both in gas phase and liquid phase. We showed the gas and liquid flow profiles, and species concentration profiles, both in the gas phase and liquid phase. The latter are highly dictated by the Henry's constants of the species. We also illustrated how the species concentrations in the liquid vary as a function of time, both during and after plasma treatment, and we explain this behavior based on the liquid phase chemistry and the Henry's constants. After plasma treatment, the concentrations of most long-lived RONS will drop within 10 seconds. The O<sub>3</sub> concentration drops linearly, and it takes ca. 50 seconds to disappear, explained by the low Henry's constant, which causes a continuous flow of O<sub>3</sub> back to the gas phase after plasma treatment. Only H<sub>2</sub>O<sub>2</sub>, HNO<sub>2</sub> and HNO<sub>3</sub> appear to be stable in the liquid after plasma treatment. Their calculated concentrations remain constant in the first 10 seconds after plasma treatment, and they will probably stay constant for a longer time as well, as confirmed by our experiments. These simulation results give us more insight in the use of PTL for cancer treatment and other medical applications.

#### 5. References

- [1] H. Tanaka, M. Mizuno, K. Ishikawa, K. Nakamura, H. Kajiyama, H. Kano, F. Kikkawa, M. Hori, Plasma-Activated Medium Selectively Kills Glioblastoma Brain Tumor Cells by Down-Regulating a Survival Signaling Molecule, AKT Kinase. *Plasma Med.* **1**, 265–277 (2011).
- [2] D. Yan, J. H. Sherman, X. Cheng, E. Ratovitski, J. Canady, M. Keidar, Controlling Plasma Stimulated Media in Cancer Treatment Application. *Appl. Phys. Lett.* **105**, 1–4 (2014).
- [3] D. Yan, N. Nourmohammadi, K. Bian, F. Murad, J. H. Sherman, M. Keidar, Stabilizing the Cold Plasma-Stimulated Medium by Regulating Medium's Composition, *Sci. Rep.* **6**, 26016 (2016).
- [4] S. Pancheshnyi, B. Eismann, G. J. M. Hagelaar, and L. C. Pitchford, University of Toulouse, LAPLACE, CNRS-UPS-INP, Toulouse, 2008.
- [5] W. Van Boxem, J. Van der Paal, Y. Gorbanev, S. Vanuytsel, E. Smits, S. Dewilde, A. Bogaerts, Anti-Cancer Capacity of Plasma-Treated PBS: Effect of Chemical Composition on Cancer Cell Cytotoxicity, *Sci. Rep.* **7**, 16478 (2017).